

Monte Carlo Simulations of Doped, Diluted Magnetic Semiconductors – a System with Two Length Scales

R. N. Bhatt and Xin Wan
*Department of Electrical Engineering, Princeton University
Princeton, New Jersey 08544, U. S. A.*

Received (received date)
Revised (revised date)

We describe a Monte Carlo simulation study of the magnetic phase diagram of diluted magnetic semiconductors doped with shallow impurities in the low concentration regime. We show that because of a wide distribution of interaction strengths, the system exhibits strong quantum effects in the magnetically ordered phase. A discrete spin model, found to closely approximate the quantum system, shows long relaxation times, and the need for specialized cluster algorithms for updating spin configurations. Results for a representative system are presented.

1. Introduction

Diluted Magnetic Semiconductors (DMS) doped with a small concentration of (shallow) charged impurities constitute an interesting magnetic system which have a number of novel features for study by numerical simulation techniques^{1,2}. These features arise because of the existence of two widely separated length scales – one of atomic dimensions ($\sim 2 \text{ \AA}$) coming from the d electrons of the magnetic ion, and the other from the effective Bohr radius of the shallow impurity, which is typically $\sim 20 \text{ \AA}$. In a certain concentration regime described below, these two lengths conspire to produce a very wide distribution of energy scales in the system, which poses special challenges for numerical simulations, in particular the problem of long equilibration times.

A prototypical DMS system is a II-VI semiconductor such as CdTe or ZnSe, which is in the zinc blende crystal structure, with some of the divalent sites (Cd/Zn) substituted by a magnetic ion, most commonly Mn. Manganese has two 4s electrons, and so is isovalent with Cd or Zn, but it also has a half filled 3d shell, which by Hund's rule, leads to a $S = 5/2$ ground state. These spins interact via a short range exchange coupling in the semiconducting (insulating) host, with nearest and second nearest neighbors usually most important. For concentrations x of Mn in, say, $\text{Cd}_{1-x}\text{Mn}_x\text{Te}$, in excess of around 0.2, the Mn spins are connected in a percolated network of short range exchange couplings, and the system is found to undergo a transition from a paramagnetic state to what is believed to be a spin glass state, at a temperature which depends on x , but is of order 10 K. For x well below that, the Mn spin system does not percolate, and the magnetic behavior is well described in

terms of predominantly isolated Mn spins, and a statistically calculable number of small clusters of Mn with typically 2, 3 or 4 Mn ions.

When shallow dopants are introduced in the system, they are characterized by a single electron or hole bound in a hydrogenic $1s$ state, the electron/hole binding energy scale being ~ 20 meV. They interact with the Mn d -electron spin via an exchange interaction of the Heisenberg type, which has a typical magnitude ~ 2 meV. Thus, it is a reasonable approximation to neglect the modification of the dopant electron (or hole^a) wavefunction by the presence of Mn spins, and the low energy Hamiltonian in the limit of low dopant density can be described as a sum of pairwise exchange interactions between the electron spins (\mathbf{s}_i) and the Mn spins (\mathbf{S}_j)³:

$$\mathcal{H} = \sum_{i,j} J(\mathbf{r}_i, \mathbf{R}_j) \mathbf{s}_i \cdot \mathbf{S}_j, \quad (1)$$

where the sum is over Mn spins at \mathbf{R}_j , and electronic spins with wavefunctions centered around the donor sites at \mathbf{r}_i . The exchange interaction energy $J(\mathbf{r}_i, \mathbf{R}_j)$ between the electron centered at \mathbf{r}_i and Mn spin at \mathbf{R}_j is proportional to the electronic charge density at the Mn site, i.e. proportional to $|\psi(\mathbf{r}_i - \mathbf{R}_j)|^2$, $\psi(\mathbf{r})$ being the ground state wavefunction of the dopant electron. (This is very much like the contact interaction between nuclear spins and electronic spins, since here the electron spin has much greater extent than the spins formed by the Mn $3d$ electrons.) For shallow donors with hydrogenic $1s$ wavefunctions, therefore,

$$J(\mathbf{r}_i, \mathbf{R}_j) = J_0 e^{-2|\mathbf{r}_i - \mathbf{R}_j|/a_B}, \quad (2)$$

where J_0 is the exchange constant and a_B the Bohr radius (~ 20 Å).

For a single dopant, this results in a polarization of the Mn spins at low temperatures in a ferromagnetic configuration with respect to each other in the absence of Mn-Mn exchange. For dilute concentration of Mn, so there are only a small fraction of near neighbor Mn clusters, we may neglect the direct Mn-Mn interaction, this magnetic polaron around each donor electron survives, and in previous work one of us has shown³ that the relative orientation of the polarons at still lower temperatures becomes ferromagnetic, as the radius of the polaron increases with lowering of T . The system would be expected to show a genuine ferromagnetic transition when the magnetic polarons percolate, so that the ferromagnetic order becomes genuinely long ranged.

However, since the percolation fraction for randomly placed spheres in three dimensions is $\sim 20\%$, even below the transition, many Mn spins remain essentially unattached to the percolated cluster till much lower temperatures. This results in a very unusual ferromagnetic phase, in which a substantial part of the spin entropy survives down to very low temperatures. Since analytic results are available only in certain limiting cases⁴, we have carried out Monte Carlo simulations of the

^aTo simplify the discussion we will consider the electron case where the electronic spin is $s = 1/2$; the hole case with spin-orbit coupling and $s = 3/2$ is more complex, but not essential for the discussion here. Therefore, we will henceforth talk only about the n -doped case.

doped DMS system for a typical dopant concentration where the isolated donor approximation for the ground state donor wavefunction would be reasonable, and a concentration of Mn where the assumption of no direct Mn-Mn interaction would be reasonable.

2. Heisenberg Model

In most magnetic models involving Heisenberg spins with large quantum numbers ($S = 5/2$ here for the Mn spins which dominate the magnetic response), quantum corrections are small and the classical vector spin model has been found to be adequate. Therefore, we performed Monte Carlo simulations on the model represented by Eqs. (1) and (2) using classical vector spins.

On a zinc-blende lattice with lattice constant of 5\AA , dopants and magnetic ions are distributed randomly on anionic and cationic sites of the lattice respectively. We choose $a_B = 20\text{\AA}$, $n_d = 10^{18}\text{cm}^{-3}$, and $x = 0.001$. The interaction between electron spins and Mn spins is antiferromagnetic. The interaction between electron spins has been shown to be unimportant³, while Mn-Mn couplings are not considered because of the rare clusters of two Mn spins on the neighboring sites ($\sim 1\%$) form a magnetically inert singlet at low temperatures. For these concentrations, Mn spins are coupled most strongly to only a few electrons, so for each Mn spin we have neglected interactions which are smaller than 10^{-5} times its strongest interaction. With this cutoff almost all Mn spins are coupled to at least two electron spins.

We carried out simulations on systems of linear sizes 20, 30, and 40, which have 256, 864, and 2048 Mn spins and 8, 27, and 64 electron spins, respectively⁶. Since we are simulating a very inhomogeneous system with large number of spins, the criterion of equilibration is crucial, especially when we try to apply the simulation to higher Mn concentrations, when clusters of many nearest neighboring Mn spins exist. Therefore, we adopt a widely used scheme in simulating spin glasses to determine the equilibration time⁵. Consider two replicas with identical locations of particles and identical couplings between them. We start one from a totally random spin configuration, and the other from a ferromagnetic configuration, in which Mn spins point in the same direction, while electron spins point opposite. We use the sample averaged magnitude of magnetization per Mn spin $\langle|M|\rangle$ as the quantity to converge. One expects that $\langle|M|\rangle$ increases from zero in the initially random replica, whereas it will decrease from the saturation value $M_0 = 5/2$ in the initially ferromagnetic replica. After $\langle|M|\rangle$ of the two replicas agree within error bars, one expects both systems have reached equilibrium, which determines the time needed before measurements can be taken.

Figure 1 shows the equilibration of a system of 864 Mn spins at $T = 0.00001$. The replica method turns out to be suitable to determine the equilibration time for the Heisenberg model even at a temperature as low as 0.00001. In the simulation, we use the standard Metropolis algorithm in which consecutive configurations can be different for no more than one single spin. At each Monte Carlo step, we go through all the spins successively and flip the spins with equilibrium probabilities.

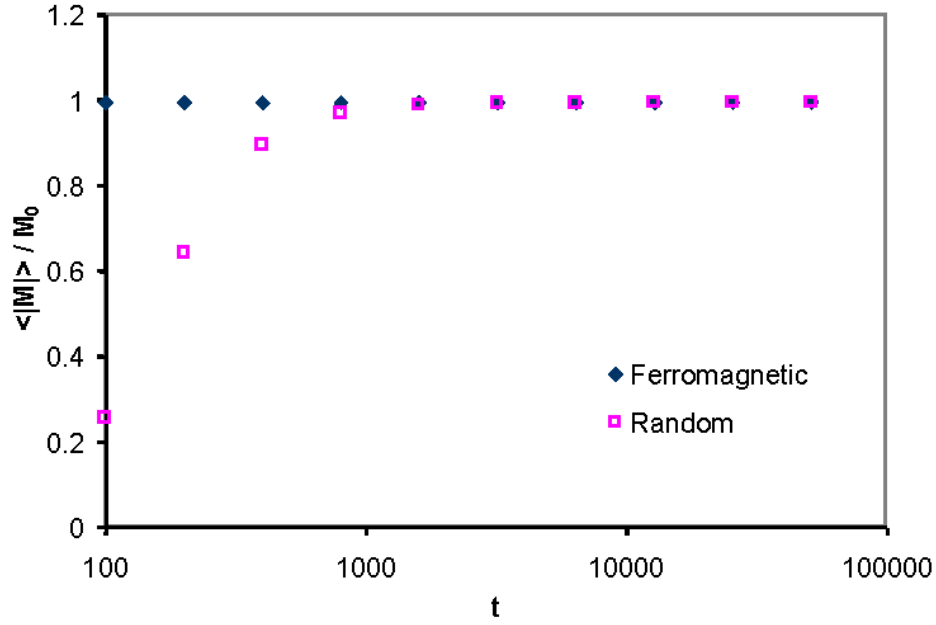


Figure 1: Sample averaged magnetization per spin M/M_0 as a function of time t for a system of 864 Mn spins at $T = 0.00001$. The upper curve evolves from ferromagnetic initial spin configuration, while the lower one evolves from random spin configuration. Classical vector spins are used in the simulation.

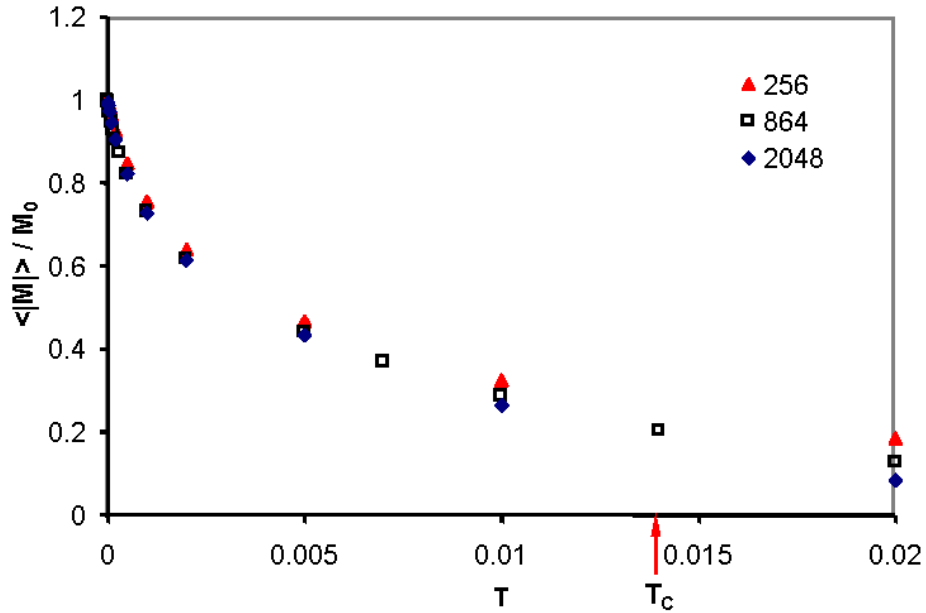


Figure 2: Normalized magnitude of magnetization per Mn spin $\langle |M| \rangle$ at different temperatures for systems of 256, 864, and 2048 Mn spins in the Heisenberg model.

Figure 2 shows the sample averaged magnitude of magnetization per Mn spin as a function of temperature for systems of 256 to 2048 Mn spins. $\langle |M| \rangle$ looks very different from that of a conventional ferromagnet. At the lowest temperatures simulated for the classical Heisenberg model, $\langle |M| \rangle$ rises steeply, approaching $M_0 = 5/2$ in a linear fashion. Magnetization per Mn spin is a good estimate of the percentage of Mn spins belonging to the percolating ferromagnetic cluster. The critical temperature $T_C \simeq 0.014$ is obtained by using various cumulants of the magnetization, which will be discussed later in Section 3 for the discrete spin model.

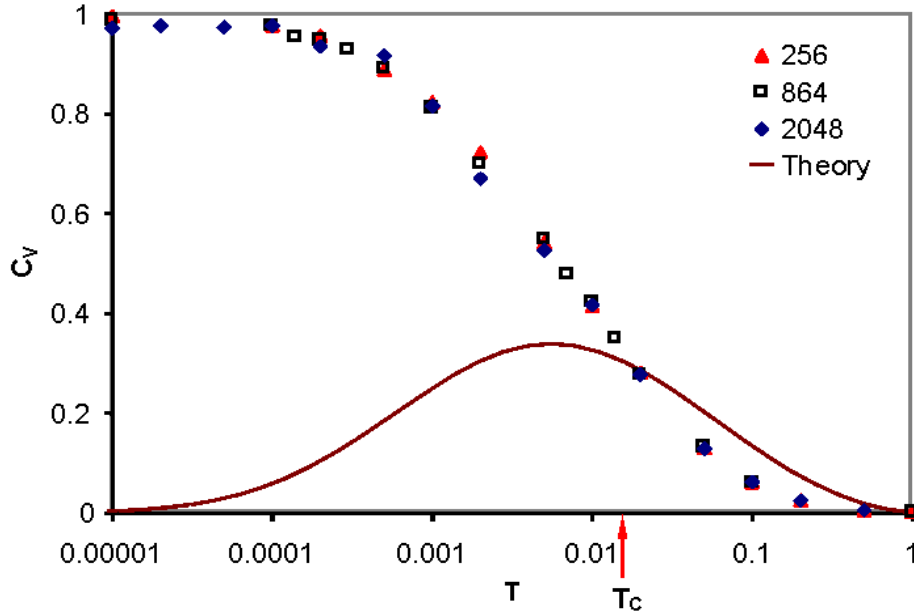


Figure 3: Specific heat C_v as a function of temperature for systems of 256, 864, and 2048 Mn spins in the Heisenberg model. The solid curve shows the theoretical estimate.

The specific heat per spin is plotted against temperature in Fig. 3. At low temperatures, C_v approaches unity which is the result of the equipartition theorem. This suggests that we cannot treat Mn spins as classical Heisenberg objects. The solid curve in Fig. 3 is a theoretical estimate of C_v for the quantum case⁴, which is expected to hold at low temperatures (only), and this clearly deviates from the simulation results below T_c and approaches zero in low temperature limit. It is noteworthy that this strong deviation between classical and quantum spins already occurs at temperatures where the magnetization is less than 40% of the saturation value. Consequently quantum effects are important in this system.

3. Discrete Spin Model

3.1. Discrete 12-state model

In order to simulate the effects of the discreteness of the quantum spins in doped diluted magnetic semiconductors without having to perform a fully quantum simulation, we have modified Mn spins from a continuous vector spin to various discrete spin versions. Here, we discuss the results of a discrete 12-state model, in which each spin can take one of the 12 $\langle 110 \rangle$ directions of a cubic lattice with a Hamiltonian given by Eqs. (1) and (2).

Figure 4(a) and (b) compare the evolution of magnetization per Mn spin in a system of 256 Mn spins at $T = 0.04$ and $T = 0.00001$ using standard single spin flip dynamics. At the higher temperature, $\langle |M| \rangle$ of the two replicas converge to the same value, implying the equilibrium is reached in both replicas. However, at temperature three orders below, the magnetization values hardly change after initial 100 steps and show no indication of equilibration. This is easily understood as follows: each single spin flip is associated with a finite energy change. Therefore, the discretization of the energy levels will inevitably lead to significant slowing down of the simulation at low temperatures. The broad distribution of interactions worsen the equilibration of discrete spins by forming domains around each electron spins where the exchanges are strong. These domains are unlikely to flip in reasonable times, because the exchanges at the domain surfaces are much weaker compared to that in the bulk. A new algorithm, which can effectively flip each domains at a single step, is thus required to achieve equilibration.

3.2. Cluster algorithm

To develop a cluster algorithm for various spin models, we follow Wolff's cluster algorithm⁷. We first define Ising-like spin-flip operation $\mathbf{s} \rightarrow \mathbf{s}'$ as the reflection with respect to the plane orthogonal to a unit vector \hat{n} ,

$$\mathcal{R}(\hat{n})\mathbf{s} = \mathbf{s} - 2(\mathbf{s} \cdot \hat{n})\hat{n}, \quad (3)$$

which satisfies

$$\mathcal{R}(\hat{n})^2 = 1, \quad (4)$$

and

$$[\mathcal{R}(\hat{n})\mathbf{s}_1] \cdot [\mathcal{R}(\hat{n})\mathbf{s}_2] = \mathbf{s}_1 \cdot \mathbf{s}_2. \quad (5)$$

In the discrete spin model, only finite number of unit vectors \hat{n} exist that transform an arbitrary discrete spin into other discrete spins. For instance, unit vectors along $\langle 110 \rangle$ and $\langle 100 \rangle$ directions are a set of appropriate reflections for discrete spins along $\langle 110 \rangle$ directions.

Due to the non-nearest-neighboring nature of spin exchanges in doped magnetic semiconductors, the cluster algorithm needs extra consideration whether the whole cluster is flipped or not. The revised cluster algorithm now consists of the following

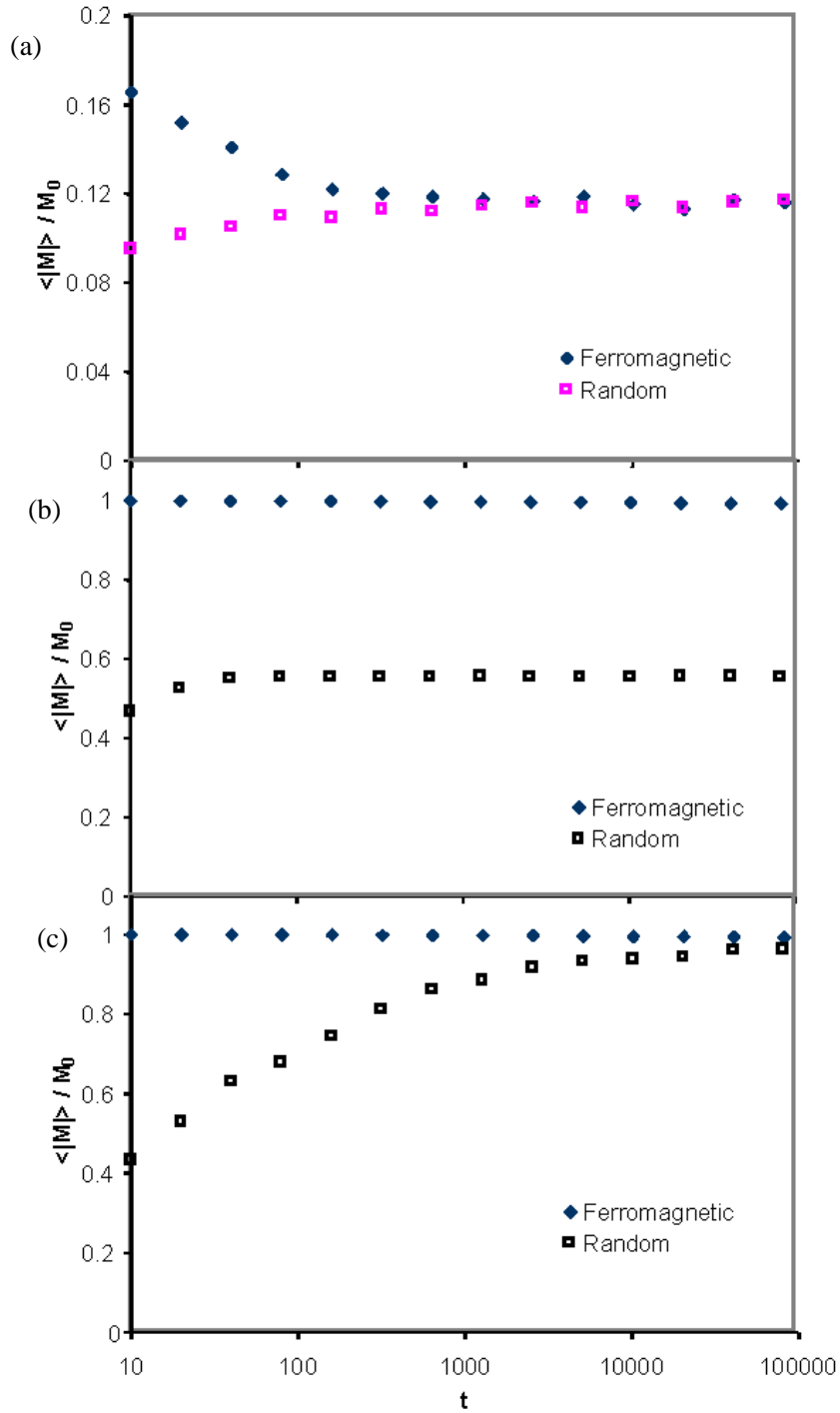


Figure 4: Magnetization per spin M as a function of time t for system with 256 Mn spins in replicas starting from ferromagnetic configuration and random configuration in the discrete 12-spin model (a) at $T = 0.04$ with single spin flips, (b) at $T = 0.00001$ with single spin flips, and (c) at $T = 0.00001$ with the cluster updating algorithm described in the text.

sequence of operations. (a) Choose a electron spin \mathbf{s}_0 at \mathbf{r}_0 and an appropriate reflection \hat{n} randomly. \mathbf{s}_0 is the seed of the cluster \mathcal{C} to be built. (b) Visit all manganese spins and activate the bond between the electron spin and a manganese spin \mathbf{S} at \mathbf{R} with probability

$$\mathcal{P}_I(\mathbf{S}) = 1 - \exp\{\min[0, 2J(\mathbf{r}_0, \mathbf{R})(\mathbf{s}_0 \cdot \hat{n})(\mathbf{S} \cdot \hat{n})/T]\}. \quad (6)$$

If the bond is activated, add \mathbf{S} to the cluster \mathcal{C} . (c) Visit all electron spins, except the seed \mathbf{s}_0 , and add an electron spin \mathbf{s} to the cluster \mathcal{C} with probability

$$\mathcal{P}_{II}(\mathbf{s}) = 1 - \exp\{\min[0, \sum_{\mathbf{S} \in \mathcal{C}} 2J(\mathbf{r}, \mathbf{R})(\mathbf{s} \cdot \hat{n})(\mathbf{S} \cdot \hat{n})/T]\}. \quad (7)$$

(d) Flip the whole cluster \mathcal{C} with probability

$$\mathcal{P}_{III}(\mathcal{C}) = \exp\{\min[0, \sum_{\mathbf{s} \in \mathcal{C} - \{\mathbf{s}_0\}, \mathbf{S} \in \mathcal{C}} 2J(\mathbf{r}, \mathbf{R})(\mathbf{s} \cdot \hat{n})(\mathbf{S} \cdot \hat{n})/T]\}. \quad (8)$$

Detailed balance is fulfilled since the transition probabilities \mathcal{W} between two configurations $\{\mathbf{s}, \mathbf{S}\}$ and $\{\mathbf{s}', \mathbf{S}'\}$ that differ by a flip $\mathcal{R}(\hat{n})$ on a cluster \mathcal{C} built around electron spin \mathbf{s}_0 obey

$$\begin{aligned} \frac{\mathcal{W}(\{\mathbf{s}, \mathbf{S}\} \rightarrow \{\mathbf{s}', \mathbf{S}'\})}{\mathcal{W}(\{\mathbf{s}', \mathbf{S}'\} \rightarrow \{\mathbf{s}, \mathbf{S}\})} &= \frac{\mathcal{P}_{III}(\mathcal{C}) \prod_{\mathbf{s} \in \mathcal{C}} [1 - \mathcal{P}_{II}(\mathbf{s})] \prod_{\mathbf{S} \in \mathcal{C}} [1 - \mathcal{P}_I(\mathbf{S})]}{\mathcal{P}_{III}(\mathcal{C}') \prod_{\mathbf{s}' \in \mathcal{C}'} [1 - \mathcal{P}_{II}(\mathbf{s}')] \prod_{\mathbf{S}' \in \mathcal{C}'} [1 - \mathcal{P}_I(\mathbf{S}')] } \\ &= \exp \left[\frac{2}{T} \left(\sum_{\mathbf{s} \in \mathcal{C} - \{\mathbf{s}_0\}, \mathbf{S} \in \mathcal{C}} + \sum_{\mathbf{s} \in \mathcal{C}, \mathbf{S} \in \mathcal{C}} + \sum_{\mathbf{s} = \mathbf{s}_0, \mathbf{S} \in \mathcal{C}} \right) J(\mathbf{r}, \mathbf{R})(\mathbf{s} \cdot \hat{n})(\mathbf{S} \cdot \hat{n}) \right] \\ &= \exp \left\{ -\frac{1}{T} \sum_{\mathbf{s}, \mathbf{S}} J(\mathbf{r}, \mathbf{R})(\mathbf{s}' \cdot \mathbf{S}' - \mathbf{s} \cdot \mathbf{S}) \right\} \end{aligned} \quad (9)$$

It is worth pointing out that all probabilities for activating bonds within \mathcal{C} are the same before or after the cluster flipping because of Eqs. (4) and (5). Due to the extremely broad distribution of spin exchanges, we add the following step to reduce the time in which all the manganese spins far away from any electron spin can reach thermal equilibrium. (e) Visit all manganese spins and flip each individual spin \mathbf{S} to an arbitrary discrete spin \mathbf{S}' with probability

$$\mathcal{P}(\mathbf{S}) = \exp\{\min[0, \sum_{\mathbf{S}'} J(\mathbf{r}, \mathbf{R})\mathbf{s} \cdot (\mathbf{S} - \mathbf{S}')/T]\} \quad (10)$$

Ergodicity of the above processes is guaranteed by the fact that there is always nonzero probability that \mathcal{C} consists of only one spin, and that there is always one reflection or two consecutive reflections connecting any two discrete spins. This allows exploration of all configurations with finite probabilities required for ergodicity.

The efficiency of the cluster algorithm can be tested at very low temperatures. Figure 4(c) shows the average evolution curve of the systems of 256 Mn spins at

$T = 0.00001$. Cluster algorithm is applied in the random replica. In 100,000 steps, $\langle |M| \rangle$ in the random replica rises to almost 97% of the value in the ferromagnetic replica. The small discrepancy largely comes from the worst 10% of the samples in which a longer time is required to remove all the domain walls.

The development of ordered state from initially random configuration particularly in systems of 256 Mn spins using cluster algorithm confirms that the replica with such ferromagnetic initial configuration can reach equilibrium by single spin-flip dynamics. Obviously, the reason is that, for the simple Hamiltonian in Eq. (1), we know that the ground state is a ferromagnetic state at zero temperature, since there is no frustration. Therefore, even if the random replica is not in equilibrium, we can measure the equilibrium quantities in the replica starting from the appropriate initial configuration after enough many steps using only single spin-flip algorithm.

Although the cluster algorithm with the replica method determining the equilibration time may appear to be a luxury in the dilute concentration limit, it is absolutely necessary when sizable clusters with Mn-Mn interactions exist at higher Mn concentrations when the ground state configuration is unknown.

3.3. Results of the discrete 12-state model

In this subsection, we show results based on the assumption that the replica starting from ferromagnetic initial configuration reaches equilibrium after long enough time, using single spin-flip dynamics.

A dimensionless quantity⁸ used to characterize the ferromagnetic order is given by

$$G_L = \frac{1}{2} \left\{ 5 - 3 \frac{\langle M^4 \rangle}{\langle M^2 \rangle^2} \right\}. \quad (11)$$

The coefficients in Eq. (11) are chosen so that G_L approaches zero in the thermodynamic limit above T_c and unity below T_c . From finite size scaling theory, we expect that G_L is size independent at the critical temperature. The three G_L curves in Fig. 5 seem to cross at $T_c \simeq 0.03$. Below T_c G_L increases as system size increases, while G_L decreases as system size increases above T_c , as expected.

The magnetization per Mn spin is plotted versus temperature for the three different system sizes in Fig 6. Compared with the results in the Heisenberg model, the curves are roughly scaled by a factor of 2 on the temperature axis, as is T_c . The specific heat per spin shown in Fig. 7 starts dropping at $T \simeq 0.001$. The simulation results in the discrete 12-state model agree quite well with the theoretical estimate for the specific heat of the quantum system⁴.

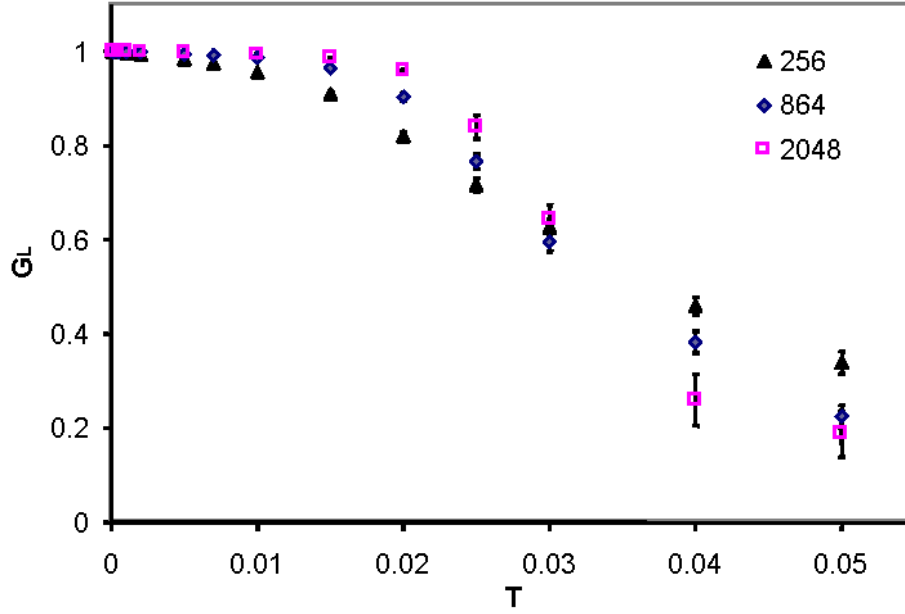


Figure 5: G_L at different temperatures for systems of 256, 864, and 2048 Mn spins in the discrete 12-state model. The crossings of the three curves indicates $T_c \sim 0.03$.

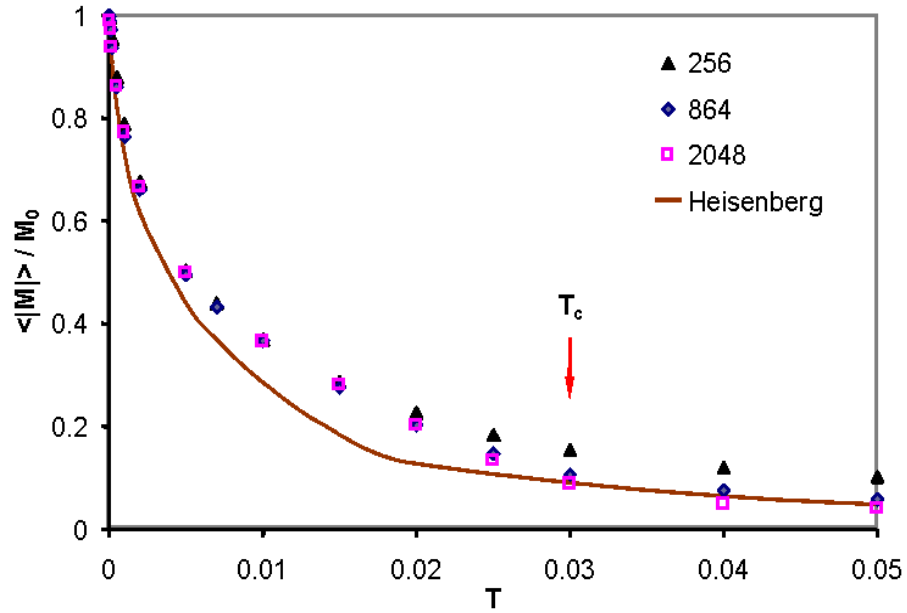


Figure 6: Normalized magnitude of magnetization per Mn spin versus temperature for different system sizes in the discrete 12-state model. The solid line fits $\langle |M| \rangle$ of the system of 864 Mn spins in the Heisenberg model.

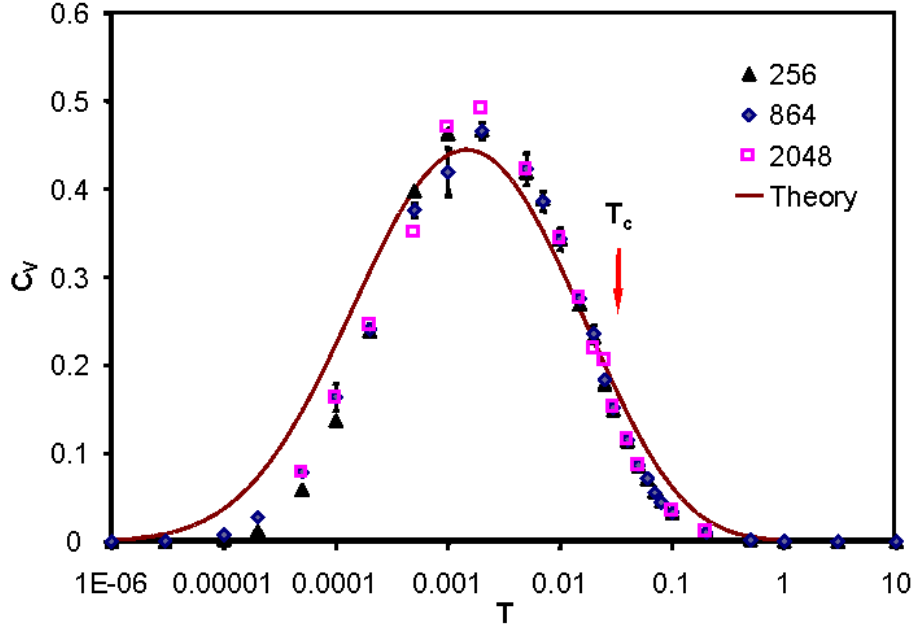


Figure 7: Specific heat C_v as a function of temperature for different system sizes in the discrete 12-state model. The solid curve is again the theoretical estimate of C_v .

4. Conclusion

In conclusion, we have presented results of a numerical simulation appropriate for diluted magnetic semiconductors with a low concentration of magnetic ions (x) and a low concentration of shallow dopants (n_d). The restriction on n_d is provided by the requirement that the system remain insulating, i.e. below the Mott concentration (or explicitly $n_d \cdot a_B^3 < 0.016$). The restriction on x is required for the Mn-dopant interaction to be the dominant interaction.

In this regime, the system is found to order ferromagnetically at low temperatures, but the ferromagnetic state is rather unusual, in that the magnetization does not approach the saturation value till well below the ordering temperature. This arises because of the effective couplings that characterize the system are distributed on a logarithmic scale owing to the exponential variation of the interactions with distance. Because of this wide distribution, the system cannot be adequately represented by a classical Heisenberg model at the low temperatures of interest. A discrete spin model is found to remove most of the inadequacies of the continuous spin model, but requires the application of specialized cluster algorithms to help alleviate the extremely long relaxation times that are inherent in a discrete spin model.

While there may be other methods to get around the problems of equilibration in the ferromagnetic regime, the cluster algorithms described above, which are

found to work well (at least for small sizes) in the concentration regimes studied, should in principle be useful in other regimes, e.g. higher Mn concentration, where Mn-Mn interactions cannot be neglected. The higher concentration regimes will involve frustration effects as well, and having a reliable numerical method to ensure equilibration is prerequisite for any study of such effects in the diluted magnetic semiconductors. We are currently testing if big enough sizes can be brought to equilibrium with the above scheme to enable finite size scaling for accurate location of T_c , and also to ensure that finite size corrections for the susceptibility, specific heat and other thermodynamic quantities in the ferromagnetic phase remain small.

Acknowledgement

This work was supported by NSF DMR 9809483.

References

1. P. A. Wolff, in *Semiconductors and Semimetals*, ed. J. K. Furdyna and J. Kossut (Academic, San Diego, 1988), Vol. 25, p. 413.
2. P. A. Wolff, in *Semimagnetic and Diluted Magnetic Semiconductors*, ed. M. Averous and B. Balkanski (Plenum, New York, 1991).
3. P.A. Wolff, R. N. Bhatt, and A. C. Durst, *J. Appl. Phys.* **79**, 5196 (1996).
4. R. N. Bhatt, *unpublished*.
5. R. N. Bhatt and A. P. Young, *Phys. Rev.* **B 37**, 5606 (1988).
6. For more details, see Xin Wan and R. N. Bhatt, *unpublished*.
7. U. Wolff, *Phys. Rev. Lett.*, **62**, 361 (1989).
8. K. Binder and A. P. Young, *Rev. Mod. Phys.* **58**, 801 (1986).